cause genome-wide dysregulation of DNA-methylation patterns that can be correlated with specific clinical outcomes[12].

Previous studies[14–16] have highlighted the diagnostic advantages of profiling DNA methylation for certain types of brain tumour because — compared with histology or the testing of specific genetic alternations — an epigenome-wide analysis of DNA methylation offers an unbiased diagnostic approach. Yet routine epigenome-wide methylation profiling remains relatively uncommon for clinical diagnosis for several reasons, including: cost; sample requirements; a shortage of staff with the necessary data-analysis expertise; and the question of whether the findings would have implications for the clinical treatments used. However, some progress is being made. For example, techniques are now available to use DNA extracted from the most common type of chemically preserved tumour tissue on glass slides, called formalin-fixed, paraffin-embedded (FFPE) specimens.

The authors provided the computer with genome-wide methylation data for samples of almost every CNS tumour type classified by the WHO. The computer used supervised machine learning to recognize methylation patterns present in the pathologist-classified samples, as well as unsupervised machine learning, which involved the computer searching the data sets for patterns that it could use to assign samples into its own computer-generated classification categories.

After training, the computer could classify tumours into 82 distinct classes on the basis of specific methylation profiles. Only 29 of these corresponded to a specific tumour type as defined by the WHO and another 29 represented subclasses of the WHO-defined tumour types.

Yet perhaps the most interesting discoveries made by Capper and colleagues were tumour classifications that grouped together histologically similar types of tumour comprising more than one tumour type as classified by the WHO, or classifications of tumour types that did not match the WHO groupings. Such discoveries might provide insight into tumour similarities that are independent of tumour histology and could aid the development of treatment options or diagnostic tools.

The authors used the computer to classify 1,104 test cases of tumours that had been diagnosed by pathologists using standard histological or molecular techniques (Fig. 1). For 60.4% of these test cases, the computer-based classification was identical to the pathologist's classification, and for 15.5% of the test cases the computer and pathologist assigned the same type of tumour but the computer could also assign the tumour into a subclass. In 12.6% of the test cases, the computer diagnosis did not match the pathologist's diagnosis. Remarkably, further rigorous analysis of these cases — by, for example, gene sequencing — resulted in the classification of 92.8% of these unmatched tumours being switched from the original clinical diagnosis to the computer-based classification. Moreover, 71% of the reclassified tumours were assigned to a different tumour grade, a recategorization that might have implications for prognosis or treatment. The remaining test cases (11.5%) could not be classified by the computer. Additional computational analysis indicates that one-third of the tumours in this group might represent rare tumours for which the computer had yet to encounter enough examples to generate a classification grouping.

Does Capper and colleagues' approach represent a probable future standard for tumour diagnosis, given the advantages, such as a low cost per sample that is comparable to that of standard cancer diagnostics; the compatibility with universally available FFPE material; and a website that facilitates data entry, analysis and tumour classification? And, if so, will histological analysis fall by the wayside?

Obtaining a comprehensive molecular profile of a tumour specimen is certainly useful, especially when combined with microscopic examination, and might be the way forward as medical treatments become ever-more personalized to the characteristics of an individual's tumour. However, for now, histology remains indispensable for disease classification because the standard approaches for specimen preservation and examination by microscopy offer the most accessible and universal entry point in the routine diagnostic workflow used in clinical laboratories worldwide. A disease can manifest itself in both molecular and cellular changes; therefore, an approach that integrates both molecular analysis and visual inspection might strengthen diagnostic capabilities.

Routine and widespread use of the platform developed by Capper *et al.* might not be practical for many laboratories at present, so the most likely immediate application of this technology would be in assessing cases with ambiguous histological characteristics. Nevertheless, Capper and colleagues' approach complements, extends and, in some cases, supersedes the tumour-diagnostic potential of microscopic examination. ■

Derek Wong *and* **Stephen Yip** *are in the Department of Pathology and Laboratory Medicine, University of British Columbia, Vancouver, British Columbia V6T 2B5, Canada.*
e-mail: stephen.yip@vch.ca

1. Capper, D. *et al. Nature* **555,** 469–474 (2018).
2. Bailey, P. & Cushing, H. *A Classification of the Tumors of the Glioma Group on a Histo-Genetic Basis with a Correlated Study of Prognosis* (Lippincott, 1926).
3. Cancer Genome Atlas Research Network. *N. Engl. J. Med.* **372,** 2481–2498 (2015).
4. Eckel-Passow, J. E. *et al. N. Engl. J. Med.* **372,** 2499–2508 (2015).
5. Sturm, D. *et al. Cell* **164,** 1060–1072 (2016).
6. Yan, H. *et al. N. Engl J. Med.* **360,** 765–773 (2009).
7. Sturm, D. *et al. Cancer Cell* **22,** 425–437 (2012).
8. Louis, D. N., Ohgaki, H., Wiestler, O. D. & Cavenee, W. K. (eds) *WHO Classification of Tumours of the Central Nervous System* 4th edn (International Agency For Research on Cancer, 2016).
9. Aldape, K., Nejad, R., Louis, D. N. & Zadeh, G. *Neuro Oncol.* **19,** 336–344 (2017).
10. Kleppe, A. *et al. Lancet Oncol.* **19,** 356–369 (2018).
11. Ehteshami Bejnordi, B. *et al. J. Am. Med. Assoc.* **318,** 2199–2210 (2017).
12. Turcan, S. *et al. Nature* **483,** 479–483 (2012).
13. Schwartzentruber, J. *et al. Nature* **482,** 226–231 (2012).
14. Wiestler, B. *et al. Acta Neuropathol.* **128,** 561–571 (2014).
15. Sahm, F. *et al. Lancet Oncol.* **18,** 682–694 (2017).
16. Korshunov, A. *et al. Acta Neuropathol.* **134,** 965–967 (2017).

This article was published online on 14 March 2018.

APPLIED PHYSICS

A diamond age of masers

Applications for masers — the microwave equivalent of lasers — have been hindered by their extreme operating conditions and the inability to produce continuous emissions. A diamond maser overcomes these limitations. SEE LETTER P.493

REN-BAO LIU

In 1954, scientists reported the first maser[1] — a device similar to a laser, but operating at microwave frequencies. Although lasers were not demonstrated until six years later[2], masers have not been as widely used as their optical counterparts. The bottleneck has been the need to operate masers under conditions of either high vacuum or extremely low temperature (a few kelvin). On page 493, Breeze *et al.*[3] present, for the first time, a maser that works continuously under ambient conditions. Such a device could lead to advances in microwave metrology and communications, and in quantum many-body physics.

The key component of a maser (or a laser) is a material known as a gain medium. In

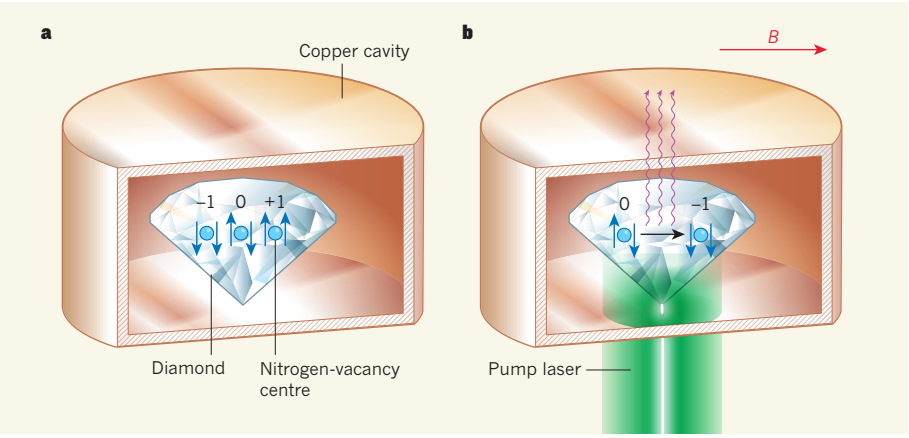

Figure 1 | A diamond maser. **a**, Breeze *et al.*[3] report a microwave laser (maser) that operates continuously under ambient conditions. Their maser consists of a closed copper structure called a cavity and a millimetre-scale diamond that contains defects known as nitrogen-vacancy centres. Each of these defects has two unpaired electrons whose magnetic moments (spins; blue arrows) can point in one of two directions. Nitrogen-vacancy centres therefore have three possible spin states (denoted by −1, 0 and +1). **b**, The authors applied a strong magnetic field (*B*) to the diamond, so that the −1 state had a lower energy than the 0 state. They then used a laser to 'pump' the nitrogen-vacancy centres into the 0 state. The defects relaxed to the −1 state (black arrow), and in doing so produced the microwave radiation associated with a maser.

ordinary materials, electrons usually exist in their lowest energy states and can absorb radiation by jumping to higher states. However, in a gain medium, the electron population is inverted: there are more electrons in higher states than in the lowest ones.

A photon passing through a gain medium can stimulate an electron in a higher state to jump to a lower state and emit an identical photon. If these photons are bounced back and forth between mirrors, or confined in a closed metal structure called a cavity, they can be copied many times before escaping from the system, generating a macroscopic quantum state of many identical photons. This process explains the name maser (laser): microwave (light) amplification by stimulated emission of radiation.

The different orientations of the tiny magnet (the spin) associated with an electron are known as electron spin states, and have energy separations of the right magnitude for microwave emission. However, these states are susceptible to the collisions, rotations and vibrations of atoms through an effect called spin–orbit coupling. Researchers have minimized atomic collisions in masers using high-vacuum conditions and dilute gain media, such as ammonia molecules (as in the first reported maser[1]), hydrogen atoms, free electrons and rubidium gases[4]. Masers have also been built using solid-state gain media, such as ruby, and sapphire 'doped' with iron, in which extremely low temperatures are required to suppress the atomic vibrations[4].

For practical applications, a solid-state maser that operates at room temperature is highly desirable. In 2012, a breakthrough towards this goal was reported in the form of a maser whose gain medium was an organic material: a crystal of the compound *p*-terphenyl, doped with pentacene molecules[5]. Lightweight atoms (such as carbon, hydrogen and oxygen) have weak spin–orbit coupling, which means that spins in organic materials have relatively long lifetimes — they can remain in a particular energy state for a long time before jumping to a different state.

Population inversion in the *p*-terphenyl maser was achieved by 'pumping' the electrons in the pentacene molecules with optical radiation at a pump rate of more than 10^4 hertz. However, organic materials cannot usually withstand the intensive laser radiation required for such optical pumping — the materials often have low melting points, are evaporated by optical radiation and have poor heat conductivity. Consequently, the *p*-terphenyl maser could produce only microwave pulses, rather than continuous emission.

Building on previous work[6–8], Breeze and colleagues used a millimetre-scale diamond as the gain medium for their maser (Fig. 1a). Because it is composed of carbon atoms, diamond would be expected to have long spin lifetimes. The authors housed the diamond in a copper cavity and introduced free-electron spins into the diamond by adding defects called nitrogen-vacancy centres. Such a defect comprises a nitrogen atom, which replaces a carbon atom, and the void of a nearest-neighbour carbon atom. A nitrogen-vacancy centre has two unpaired electrons and three possible spin states (denoted by −1, 0 and +1)[9].

Breeze *et al.* applied a strong, uniform magnetic field to the diamond so that the −1 state had a lower energy than the 0 state. They then used a laser to pump the nitrogen-vacancy centres into the 0 state, to achieve population inversion. The defects produced microwave radiation as they relaxed to the −1 state (Fig. 1b).

The maser required a pump power of at least 138 milliwatts. For a power of 180 mW, the authors measured the spin lifetime of the nitrogen-vacancy centres to be roughly 50 times that of the electrons in the *p*-terphenyl maser and the pump rate to be only about 300 Hz. Thanks to diamond's high thermal conductivity (10,000 times higher than that of *p*-terphenyl), the temperature of the gain medium increased by only 35 °C when the pump power was raised to 400 mW. At room temperature, the maser worked continuously for up to 10 hours without noticeable degradation in power.

Because the frequency of microwaves produced by masers is highly stable, these devices have applications in time-keeping, high-precision spectroscopy and microwave amplification for deep-space communication and for the detection of astronomical objects. In the absence of solid-state masers that could operate at room temperature, alternative microwave sources and amplifiers were developed that were based on, for example, electronic circuits called crystal oscillators[10] and sensitive detectors known as superconducting quantum-interference devices[11]. These usually also require low temperatures. The authors' room-temperature solid-state maser could therefore transform both microwave metrology and communications.

The good thermal conductivity of diamond and the persistence of long spin lifetimes at high temperatures[12] mean that the authors' maser could be pumped at higher powers than they demonstrated, improving both the intensity and the stability of the emission. However, the maser's performance is constrained by various factors, including the requirement for a strong, uniform magnetic field, temperature fluctuations caused by laser heating and low efficiency of power conversion from the pump laser to the output. Possible approaches to address these issues could include introducing the types of defect found in similar materials to diamond[8], or borrowing ideas from other areas of research, such as superradiant lasers[13] and lasing without population inversion[14].

Finally, Breeze and colleagues' maser could provide a platform for studying quantum many-body physics. The spins of nitrogen-vacancy centres have not only long lifetimes, but also long coherence times[9] — the length of time for which spins can be in several different energy states at the same time, known as a quantum superposition. For this reason, nitrogen-vacancy centres have been intensively studied for quantum computing[9] and quantum sensing[15].

The interaction between many spins and many microwave photons in the authors' maser could result in a quantum mixture that has a half-spin, half-photon nature[16–18]. Such a mixture might offer a way to study macroscopic quantum phenomena at room

temperature. These studies could be further enriched by introducing dipole–dipole interactions between the spins, or by transforming the electron spin states into nuclear spin states.

Moreover, if the spin coherence time in the maser were longer than the photon storage time of the cavity, a photon–spin mixture could be realized in which the quantum coherence is associated mainly with the spins. The result would be a superradiant maser[13] that, unlike the authors' maser, has an emission frequency that is insensitive to the temperature fluctuations caused by laser heating. Thanks to Breeze and colleagues, a diamond age of masers can now be envisaged. ■

Ren-Bao Liu *is in the Department of Physics and the Centre for Quantum Coherence, The Chinese University of Hong Kong, Shatin, New Territories, Hong Kong, China.*
e-mail: rbliu@cuhk.edu.hk

1. Gordon, J. P., Zeiger, H. J. & Townes, C. H. *Phys. Rev.* **95,** 282–284 (1954).
2. Maiman, T. H. *Nature* **187,** 493–494 (1960).
3. Breeze, J. D., Salvadori, E., Sathian, J., Alford, N. McN. & Kay, C. W. M. *Nature* **555,** 493–496 (2018).
4. Bertolotti, M. *The History of the Laser* (CRC, 2004).
5. Oxborrow, M., Breeze, J. D. & Alford, N. M. *Nature* **488,** 353–356 (2012).
6. Jin, L. *et al. Nature Commun.* **6,** 8251 (2015).
7. Poklonski, N. A. *et al. Chin. Phys. Lett.* **24,** 2088–2090 (2007).
8. Kraus, H. *et al. Nature Phys.* **10,** 157–162 (2014).
9. Doherty, M. W. *et al. Phys. Rep.* **528,** 1–45 (2013).
10. van Beek, J. T. M. & Puers, R. *J. Micromech. Microeng.* **22,** 013001 (2012).
11. Clarke, J. & Braginski, A. I. (eds) *The SQUID Handbook: Fundamentals and Technology of SQUIDs and SQUID Systems* Vol. I (Wiley, 2004).
12. Toyli, D. M. *et al. Phys. Rev. X* **2,** 031001 (2012).
13. Bohnet, J. G. *et al. Nature* **484,** 78–81 (2012).
14. Scully, M. O., Zhu, S.-Y. & Gavrielides, A. *Phys. Rev. Lett.* **62,** 2813–2816 (1989).
15. Schirhagl, R., Chang, K., Loretz, M. & Degen, C. L. *Annu. Rev. Phys. Chem.* **65,** 83–105 (2014).
16. Zhang, X., Zou, C.-L, Jiang, L. & Tang, H. X. *Phys. Rev. Lett.* **113,** 156401 (2014).
17. Tabuchi, Y. *et al. Phys. Rev. Lett.* **113,** 083603 (2014).
18. Rose, B. C. *et al. Phys. Rev. X* **7,** 031002 (2017).

NEURODEGENERATION

Protein aggregates caught stalling

Low-complexity protein aggregates are a hallmark of neurodegeneration. High-resolution snapshots of the structure of one such aggregate offer an unprecedented view of how these proteins disrupt crucial cellular functions.

LAURA PONTANO VAITES & J. WADE HARPER

Neurodegenerative diseases are often associated with genetic mutations that cause repetition of short sequences of nucleotides. In the disorders amyotrophic lateral sclerosis (ALS, also known as motor neuron disease) and frontotemporal dementia, such an expansion in a non-protein-coding region of the *C9orf72* gene[1,2], leads to aberrant translation products that contain repetitive stretches of glycine and alanine amino-acid residues. These 'poly(GA)' products form aggregates in neurons, and have been implicated in the disruption of a key cellular process in which complexes called proteasomes degrade proteins[3,4]. However, the biochemical basis for this disruption, and how it might promote disease, is poorly understood. Writing in *Cell*, Guo *et al.*[5] precisely map the organizational and structural features of poly(GA) aggregates and associated macromolecular complexes in neurons using a technique called 3D cryo-electron tomography (cryo-ET), to provide direct visualization of how proteasomes are disrupted by poly(GA) proteins.

Cryo-ET in 3D uses electron microscopy to view very thin, frozen but hydrated sections of a cell from various angles. The resulting images are combined to produce a 3D image called a tomogram. Guo *et al.* used 3D cryo-ET to visualize neurons that had been genetically engineered to express a poly(GA) tract that contained either 175 or 73 repeats. The tracts were fused with a green fluorescent protein that enabled their precise position to be determined using correlative light microscopy. The engineered protein mimics poly(GA) tracts that are produced from *C9orf72* expansion, which take a long time to form *in vivo*. The authors found that poly(GA) proteins form highly clustered and often bifurcated twisted ribbon structures that are of relatively uniform thickness, but of variable length and width, similar to poly(GA) structures previously observed by conventional electron microscopy *in vitro*[6].

The value of the authors' work lies not only in their observation of the structure of poly(GA) aggregates in detail in cells, but in their comparison of poly(GA) with aggregates formed through a different genetic expansion — a glutamine repeat (poly(Q)) tract, which causes the neurodegenerative disorder Huntington's disease, and which the same group analysed by 3D cryo-ET last year[7]. This comparison revealed structural differences that could explain dissimilarities in pathogenic mechanisms between the conditions.

First, the aggregates formed in each case are themselves structurally distinct. Poly(Q) proteins form fibril structures that show little

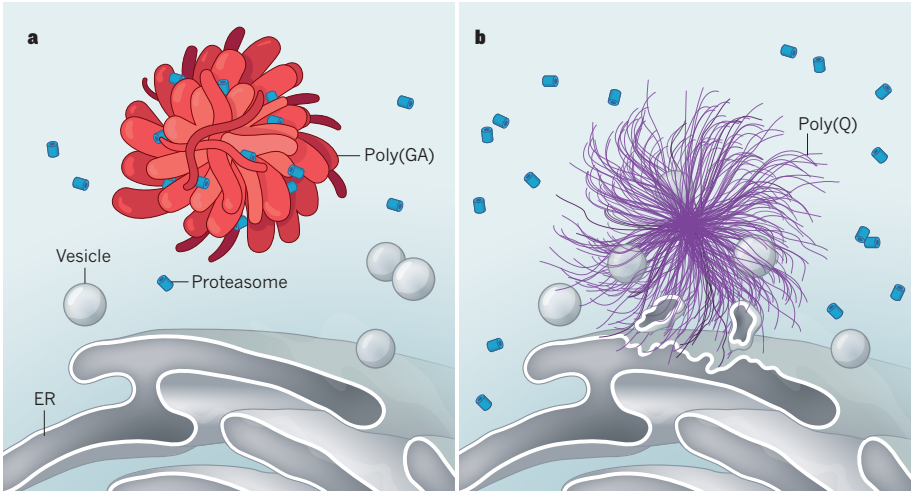

Figure 1 | Contrasting mechanisms of aggregate toxicity. a, In some cases of the neurodegenerative disorder amyotrophic lateral sclerosis, long chains of glycine and alanine amino-acid residues (dubbed poly(GA) tracts) aggregate in neurons. Guo *et al.*[5] show, through high-resolution structures in cells, that poly(GA) tracts form ribbon-like aggregates that capture protein complexes called proteasomes, which normally process other proteins for degradation. Such capture causes proteasome stalling, providing an explanation for the toxicity of this aggregate. Poly(GA) aggregates do not bind membrane-bound organelles such as vesicles and the endoplasmic reticulum (ER). **b**, By contrast, repetitive tracts of the amino acid glutamine (poly(Q) tracts), which are associated with Huntington's disease, form fibril-like aggregates[7]. These aggregates deform the membranes of vesicles and the ER, suggesting that different aggregates cause neurodegeneration through different mechanisms.